JACS
JOURNAL OF THE AMERICAN CHEMICAL SOCIETY
Article
pubs.acs.org/JACS

Quest for Highly Connected Metal–Organic Framework Platforms: Rare-Earth Polynuclear Clusters Versatility Meets Net Topology Needs

Dalal Alezi,[†] Abdul Malik P. Peedikakkal,[†] Łukasz J. Weseliński,[†] Vincent Guillerm,[†] Youssef Belmabkhout,[†] Amy J. Cairns,[†] Zhijie Chen,[†] Łukasz Wojtas,[‡] and Mohamed Eddaoudi*[,†]

[†]Functional Materials Design, Discovery and Development Research Group (FMD[3]), Advanced Membranes and Porous Materials Center, Division of Physical Sciences and Engineering, King Abdullah University of Science and Technology (KAUST), Thuwal 23955-6900, Kingdom of Saudi Arabia

[‡]Department of Chemistry, University of South Florida, 4202 East Fowler Avenue, Tampa, Florida 33620, United States

Supporting Information

ABSTRACT: Gaining control over the assembly of highly porous rare-earth (RE) based metal–organic frameworks (MOFs) remains challenging. Here we report the latest discoveries on our continuous quest for highly connected nets. The topological exploration based on the noncompatibility of a 12-connected RE polynuclear carboxylate-based cluster, points of extension matching the 12 vertices of the cuboctahedron (**cuo**), with 3-connected organic ligands led to the discovery of two fascinating and highly connected minimal edge-transitive nets, **pek** and **aea**. The reduced symmetry of the employed triangular tricarboxylate ligand, as compared to the prototype highly symmetrical 1,3,5-benzene-(tris)benzoic acid guided the concurrent occurrence of nonanuclear $[RE_9(\mu_3\text{-}OH)_{12}(\mu_3\text{-}O)_2(O_2C-)_{12}]$ and hexanuclear $[RE_6(OH)_8(O_2C-)_8]$ carboxylate-based clusters as 12-connected and 8-connected molecular building blocks in the structure of a 3-periodic **pek**-MOF based on a novel (3,8,12)-c trinodal net. The use of a tricarboxylate ligand with modified angles between carboxylate moieties led to the formation of a second MOF containing solely nonanuclear clusters and exhibiting once more a novel and a highly connected (3,12,12)-c trinodal net with **aea** topology. Notably, it is the first time that RE-MOFs with double six-membered ring (d6R) secondary building units are isolated, representing therefore a critical step forward toward the design of novel and highly coordinated materials using the supermolecular building layer approach while considering the d6Rs as building pillars. Lastly, the potential of these new MOFs for gas separation/storage was investigated by performing gas adsorption studies of various probe gas molecules over a wide range of pressures. Noticeably, **pek**-MOF-1 showed excellent volumetric CO_2 and CH_4 uptakes at high pressures.

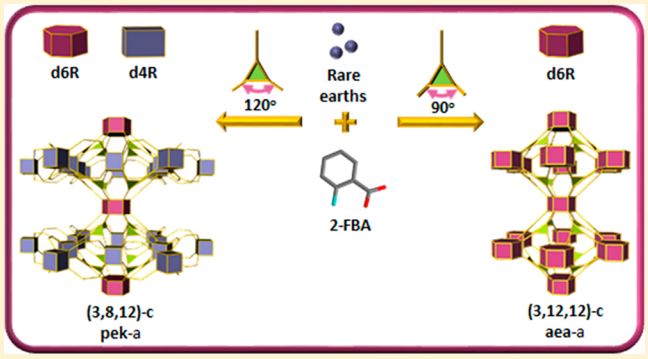

INTRODUCTION

Metal–organic frameworks (MOFs) are considered nowadays as the most promising class of porous materials that are positioned to address many enduring societal challenges pertaining to energy and environmental sustainability, due to the prospective ability to mutually control their porous system structure, composition, and functionality.[1,2] The inherent structural modularity (e.g., use of different metals, extensive library of organic building blocks with various shapes and dimensions, postsynthetic modifications, etc.) and exceptional controlled porosity place MOFs as ideal candidate materials for various relevant applications such as gas separation, gas storage, drug delivery, catalysis and chemical sensing.[1c−f] However, the rational understanding of their assembly is still in its infancy, and as such many paths remain to be explored to facilely achieve in the near future made-to-order MOFs, stable materials specifically designed for particular applications.[2]

The systematic use of the topology tool[3] and the Reticular Chemistry Structural Resource (RCSR) database,[4] often not universally recognized, has permitted the successive establishment of several powerful design strategies, such as the molecular building block (MBB),[1a] the supermolecular building block (SBB),[2,5] and more recently the supermolecular building layer (SBL)[2,6] approaches.

Evidently, highly connected and minimal-edge transitive nets are of a prime interest in crystal chemistry, and can be regarded as ideal blueprints for the rational design and construction of MOFs. Reasonably, the assembly of highly connected building blocks offer prospective to limit/reduce the number of plausible resultant networks—nets with at least one n-connected node where $n \geq 12$ represent only 2.7% of the nets reported in the

Received: January 20, 2015
Published: April 7, 2015

DOI: 10.1021/jacs.5b00450
J. Am. Chem. Soc. 2015, 137, 5421−5430

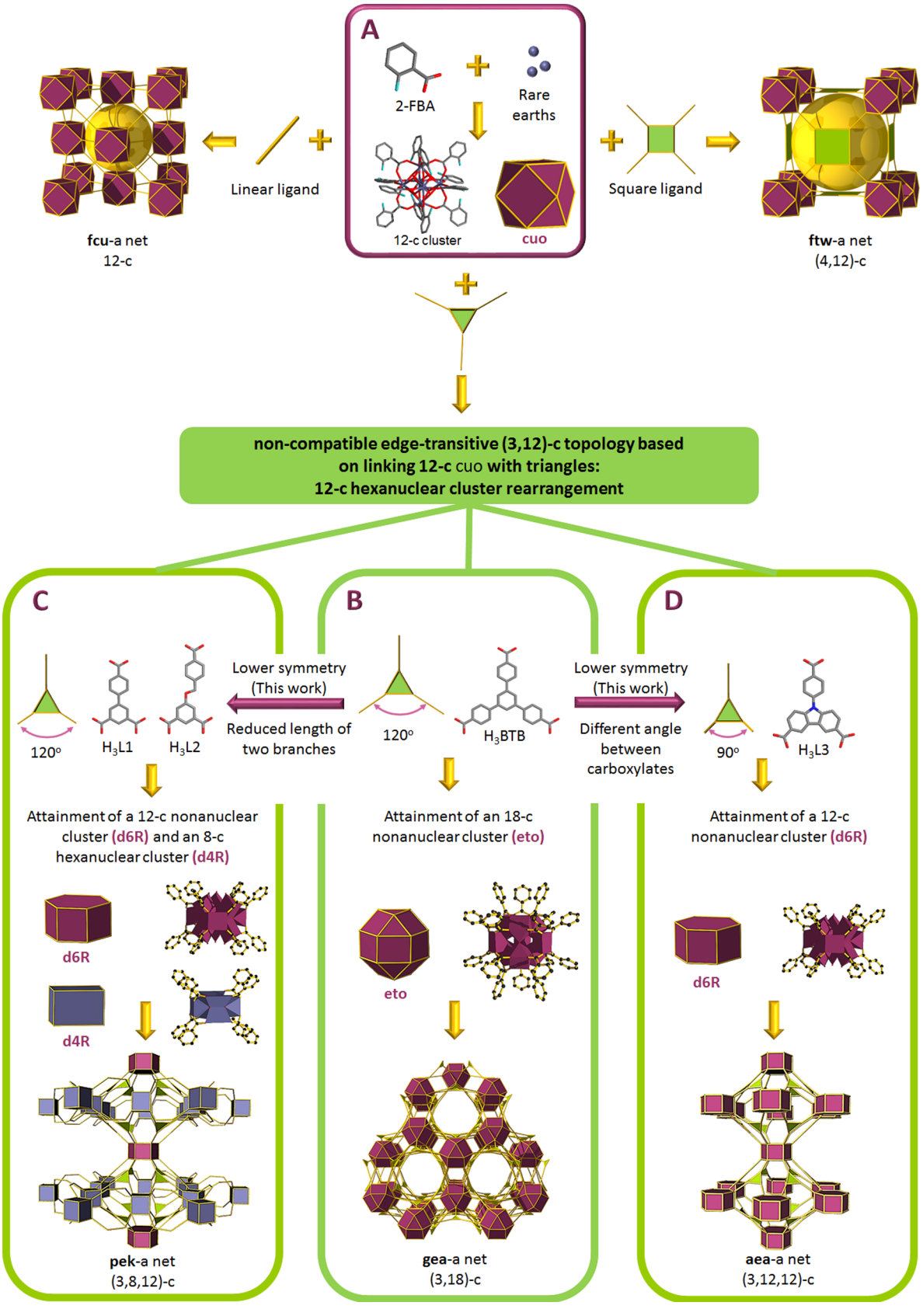

Figure 1. Illustration of the topological exploration path: (A) The discovery of a 12-c RE hexanuclear cluster and its logical assembly into **fcu**-MOFs (upper left) and **ftw**-MOFs (upper right). (B) Employment of a symmetrical 3-c ligand prompted the formation of a novel 18-c nonanuclear cluster and its reticulation into a new highly connected (3,18)-c **gea** net. (C,D) Use of a less symmetrical 3-c ligands lead to the discovery of a (3,8,12)-c **pek** net and a (3,12,12)-c **aea** net, respectively. Nets are represented in their augmented forms for better illustration and understanding.

DOI: 10.1021/jacs.5b00450
J. Am. Chem. Soc. 2015, 137, 5421−5430

RCSR database.[5] The occurrence of said highly connected MBBs (n-connected where $n \geq 12$) in the open literature still remains elusive,[5c,7] mainly because of the fact that MBBs with corresponding high-connectivity are often too intricate to be attained as polynuclear clusters.

Given this critical limitation and considering our recent contributions on highly connected RE-MOFs,[5c,7h] where we unveiled the versatility of RE polynuclear clusters leading in the presence of given polytopic ligands to the construction of 12-c and unprecedented 18-c porous RE-MOFs, on the basis of distinctive highly coordinated RE hexanuclear and nonanuclear carboxylate-based clusters, respectively, we aim to further exploit this unforeseen induced adaptability of RE polynuclear clusters by the geometry and connectivity of linkers as a route for the discovery of highly connected MBBs and/or new highly connected nets. Markedly, our group has succeeded in controlling the directionality of RE based inorganic MBBs by pioneering the use of fluorinated ligands and/or a modulators such as 2-fluorobenzoic acid (2-FBA).[7h] This strategy is used not only to promote the crystallization of the resultant MOF materials,[8] but most also importantly to preclude the formation of the RE based inorganic chains, dominant infinite building units in RE-MOF chemistry due to the RE hard sphere behavior that offers only limited possibilities to control the directionality and dimensionality of coordinated carboxylate-based ligands.[9]

Accordingly, by implementing our approach we isolated unprecedented highly connected porous RE-MOFs, based on highly coordinated hexanuclear and nonanuclear carboxylate-based clusters.[5c,7h] Namely, predetermined reaction conditions that consistently allow in situ formation of the RE hexanuclear cluster, $[RE_6(\mu_3\text{-}OH)_8(O_2C-)_{12}]$ acting as a 12-c MBB, were employed to construct (i) isoreticular **fcu**-MOFs[7h] when linear ligands are bridging the resultant 12-c cuboctahedron (**cuo**) secondary building units (SBUs), and (ii) isoreticular **ftw**-MOFs when the 12-c **cuo** SBUs were linked by 4-c square shaped ligands.[10] It is worth noting that we employ the term MBB when we refer to the chemical composition of a given building block and the conceptual term SBU when we point to the building block resultant geometry and connectivity upon joining its points of extension.

Subsequently, reaction conditions that formerly allowed the isolation of **fcu**-MOFs, now, in the presence of the triangular 1,3,5-benzene(tris)benzoate (BTB) ligand, have permitted the introduction for the first time of (i) a novel RE nonanuclear carboxylate-based cluster $[RE_9(\mu_3\text{-}OH)_8(\mu_2\text{-}OH)_3(O_2C-)_{18}]$ (RE = Y, Tb, Er, Eu), generated in situ, serving as an 18-connected MBB and (ii) an unprecedented **gea**-MOF based on the assembly of the subsequent 18-c **eto** and 3-c triangular SBUs.[5c] The gratifying discovery of the (3,18)-c minimal-edge transitive net, **gea**-net, was a result of our continuous commending credence that a reasonable understanding of basic topological possibilities for the assembly of high-symmetry building blocks, in combination with the required chemical skill, offers unparalleled prospective for the design, discovery and synthesis of new structures.[1a,11] Notably, minimal-edge transitive nets are suitable targets in MOF crystal chemistry; structures with high-symmetry topologies will be the most overriding resultant structures.

Practically, a key prerequisite for the successful implementation of the MBB approach for the rational design and construction of MOFs, and subsequently the practice of isoreticular chemistry, is the isolation of the reaction conditions that consistently allow the in situ formation of the desired inorganic MBB, matching the augmented basic building units (vertex figures) of the targeted net. Conceivably, the combination of the said 12-c MBB with a 3-connected rigid, directional and geometrically noncompatible organic building block, under similar reaction conditions permitting the construction of isoreticular **fcu**-MOFs and **ftw**-MOFs, promoted the adaptability of the RE hexanuclear cluster into an 18-c RE nonanuclear cluster and subsequently the discovery of the unprecedented (3,18)-c MOF.[5c] The deliberate choice of the 3-connected triangular ligand was founded by our comprehensive analysis of the RSCR database, revealing the absence of any enumerated minimal-edge transitive net for the assembly of 12-c **cuo** SBU and 3-c ligand (triangular SBU), suggesting the plausible incompatibility/mismatch of the aforementioned building units.[5]

The prompted discovery of the (3,18)-c net and the evident versatility of polynuclear RE carboxylate-based clusters have inspired us to expand this approach, based on building units mismatch, to other polytopic ligands with the main aim to uncover new highly connected MOFs.

Noticeably, careful examination of the resultant (3,18)-c net revealed the necessity to employ definite triangular organic building units, where the carbon of the carboxylate moieties as points of extension match the vertices of an equilateral triangle, in order to effectively space and arrange the 18-c MBBs in the requisite ABA hexagonal close-packing and subsequently construct the anticipated isoreticular **gea**-MOFs. Presumably, distortion of the **gea**-a requisite symmetrical triangular building unit, i.e., expansion of the symmetrical triangular **gea** vertex figure in one direction via employing a relatively less symmetrical triangular organic building unit, where the carbon of the carboxylate moieties match the vertices of an isosceles triangle (two equal sides and two equal angles), will disrupt the ABA hexagonal close-packing necessary for the attainment of the pertinent (3,18)-c isoreticular **gea**-MOFs. Therefore, this will conceivably promote the adaptability of the resultant RE polynuclear carboxylate-based cluster to match the distinct imposed 3-connected ligand geometrical attributes and the subsequent construction of a cooperative highly connected RE-MOF.

Indeed reaction conditions that formerly allowed the isolation of **fcu**-MOF, **ftw**-MOF and **gea**-MOF platforms, now, in the presence of less symmetrical 3-c ligands biphenyl-3,4,5-tricarboxylic acid ($\mathbf{H_3L1}$) and 9-(4-carboxyphenyl)-9*H*-carbazole-3,6-dicarboxylic acid ($\mathbf{H_3L3}$) (Figure 1), have permitted for the first time (i) the establishment a novel RE hexagonal prismatic SBU, a new 12-connected RE nonanuclear carboxylate-based cluster MBB and (ii) the formation of two highly connected MOF platforms, **pek**-MOF and **aea**-MOF, based on two newly revealed minimal edge-transitive nets, i.e., (3,8,12)-c net = **pek** topology and (3,12,12)-c net = **aea** topology.

RESULTS AND DISSCUSION

pek-MOF Platform. At the outset of this study, reactions of $\mathbf{H_3L1}$ with lanthanides yielded relatively dense MOF structures, with modest porosity, based on the restrained assembly of low-connectivity Ln-MBBs (i.e., less than 8-connected) or on the rod-packing of Ln-extended building units (chains), regulated by lanthanide ions high coordination numbers and associated hard acid character.[12] Nevertheless, our recent reports on RE-MOF chemistry reveal the ability to readily access highly

DOI: 10.1021/jacs.5b00450
J. Am. Chem. Soc. 2015, 137, 5421−5430

connected RE-MOFs, widely open porous structures, based on a unique methodology involving the use of 2-fluorobenzoic acid (2-FBA) as a modulator and a directing agent for the *in situ* formation of highly connected polynuclear carboxylate-based clusters.[5c,7h] Reasonably, the systematic re-exploration of previously studied rare earth metal/ligand systems in the presence of 2-FBA offer prospective for the discovery of novel highly connected RE-MOFs.[5c]

Indeed, solvothermal reaction between **H_3L1** and $Tb(NO_3)_3 \cdot 5H_2O$ in an *N*,*N*′-dimethylformamide (DMF)/water/chlorobenzene solution and in the presence of 2-FBA yielded transparent hexagonal crystals, formulated by single-crystal X-ray diffraction (SCXRD), elemental microanalysis, NMR and water adsorption studies as follows:

$|(DMA)_7|[(Tb_9(\mu_3\text{-}OH)_{12}(\mu_3\text{-}O)_2(H_2O)_9)(Tb_6(\mu_3\text{-}OH)_8(2\text{-}FBzoate)_2(HCO_2)_2(H_2O)_{4.5})_3(\mathbf{L1})_{12}]\cdot(solv)_x$ (**1**); (DMA = dimethylammonium cations, solv = solvent, **L1** = $C_{15}H_7O_6$, 2-fluorobenzoate (2-FBzoate) = $C_7H_4FO_2$).

The SCXRD study discloses that compound **1** crystallizes in a primitive hexagonal space group, *P6*/*mmm*. Analysis of the resultant crystal structure of **1** reveals the *in situ* formation of two highly connected and distinct terbium (Tb) polynuclear carboxylate-based clusters, namely an 8-c Tb hexanuclear cluster and a 12-c Tb nonanuclear cluster, and their subsequent copolymerization by the fully deprotonated tricarboxylate ligands (**L1**) to yield a novel 3-periodic highly connected Tb-MOF.

Analysis of the Tb hexanuclear cluster reveals that two Tb ions are each coordinated to nine oxygen atoms; namely, four carboxylates from four separate **L1** ligands, four μ_3-OHs and one terminal water molecule. The remaining four Tb ions are each coordinated to eight oxygen atoms; that is, four from carboxylates of four independent **L1** ligands, and the other four coordination sites are completed by oxygen atoms from bridging μ_3-OHs and disordered terminal ligands (i.e., 2-FBzoate, formate and water). Concisely, the resultant hexanuclear cluster, $[Tb_6(\mu_3\text{-}OH)_8(O_2C-)_8(O_2C-C_6H_4F)_2(O_2C-H)_2(H_2O)_{4.5}]$, is capped by 8 carboxylates from 8 different **L1** ligands (Figure 1) and 4 carboxylates from four terminal ligands (evenly 2-FBzoate and formate anions) to give an 8-connected MBB, $[Tb_6(\mu_3\text{-}OH)_8(O_2C-)_8]$, with points of extension corresponding to carbons of the carboxylate moieties from eight distinct tricarboxylate ligands and matching the d4R vertex figure of a fully symmetrical 8-connected node.

Similarly, inspection of the Tb nonanuclear cluster unveils that six Tb ions are coordinated to eight oxygen atoms (that is, two from carboxylates of two separate **L1** ligands, four μ_3-OH, two μ_3-O and one from a terminal water molecule), and that the remaining three Tb ions are coordinated each to nine oxygen atoms (namely, four from carboxylates of four separate **L1** ligands, four μ_3-OH and one from a terminal water molecule). Distinctly, the nonanuclear cluster, $[Tb_6(\mu_3\text{-}OH)_8(\mu_3\text{-}O)_2(O_2C-)_{12}(H_2O)_9]$, is capped by 12 carboxylates from 12 different **L1** ligands (Figure 1) to give a new 12-connected MBB, $[Tb_9\ (\mu_3\text{-}OH)_{12}(\mu_3\text{-}O)_2(O_2C-)_{12}]$, with points of extension corresponding to carbons of the carboxylate moieties from 12 distinct tricarboxylate ligands and providing the hexagonal prism arrangement, matching the d6R vertex figure of a 12-connected node with a 6-fold symmetry.

Appreciably, the combination of the aforementioned 12-c MBB, $[Tb_9\ (\mu_3\text{-}OH)_{12}(\mu_3\text{-}O)_2(O_2C-)_{12}]$, and 8-c MBB, $[Tb_6(\mu_3\text{-}OH)_8(O_2C-)_8]$, with the 3-c tricarboxylate ligand resulted in the formation of an unprecedented highly connected Tb-MOF with a (3,8,12)-connected net and **pek** underlying topology, Tb-**pek**-MOF-1 (Figure 1). It is worth noting that the newly explored trinodal **pek** net has the transitivity [3244], a minimal edge transitive net with only two edges. Appropriately, **pek** net can categorized as a suitable blueprint for the design of MOFs.

Markedly, the projected versatility of RE polynuclear clusters has permitted the isolation and introduction of two key highly connected MBBs, namely the d4R SBU and most decisively the d6R SBU, looked-for in MOF crystal chemistry and deemed appropriate for the effective practice of reticular chemistry.

Our recent study on highly connected RE-MOFs postulated the plausible relationship between the 12-connected RE hexanuclear and the 18-connected RE nonanuclear clusters observed in **fcu**-MOFs[7h] and in the **gea**-MOF-1,[5c] respectively. Observably, the triangular ligand geometrical attributes and subsequent net incompatibility have prompted the incorporation of three additional RE metal ions in the hexanuclear 12-c MBB (**cuo**) to afford the accommodation of six additional peripheral carboxylate moieties from the 3-c bridging ligands, thus resulting in the perceived cluster evolution to a nonanuclear 18-c MBB (**eto**) (Figure 1). The Tb-**pek**-MOF-1 discloses another intriguing facet enriching the adaptability of the RE polynuclear clusters. Namely, the attainment of the first (3,8,12)-c RE-MOF, the **pek**-MOF-1, illustrates the attractive prospective to reduce the points of extension (n-connectivity) in the parent RE hexanuclear (**cuo**) and the RE nonanuclear clusters (**eto**). Specifically, in the hexanuclear cluster four of the 12 carboxylate moieties from the bridging ligands, originally connecting and acting as points of extension in the **fcu**-MOFs, are substituted by carboxylates from terminal ligands (2-FBzoate and formate anions), thus affording the remaining eight connecting carboxylates' arrangement in a cube-like fashion, d4R. The d4R building unit, commonly occurring in conventional inorganic zeolites, was employed effectively to target and construct zeolite-like MOFs (ZMOFs).[13]

Interestingly, in the **pek**-MOF-1 nonanuclear cluster all the 12 coordinating carboxylate moieties, capping the cluster and arranged in an hexagonal prism fashion (d6R), belong solely to the 3-connected bridging ligands and thus suggesting the plausible occurrence of the nonanuclear cluster and its rearrangement to accommodate only 12 coordinating carboxylates, in contrast to nonanuclear 18-c MBB observed in the **gea**-MOF-1 where the 18 coordinating carboxylate moieties capping the polynuclear cluster are from bridging ligands (Figure S8, Supporting Information).

The isolation of the **pek**-MOF-1 has permitted the enclosure of two additional RE-MBBs (d4R and d6R SBUs) in the repertoire of highly connected RE-MBBs. To the best of our knowledge, based on the open literature search and the Cambridge Structural Database (CSD) analysis,[14] the aforementioned hexagonal prism building unit (d6R) has never been observed in MOFs as a nonanuclear carboxylate-based cluster. However, while writing this paper, a zirconium hexanuclear carboxylate-based cluster was reported to act as a d6R SBU to form a **shp**-MOF when combined with a square-like tetratopic carboxylate ligand.[15] It is worth noting that variation of the hexanuclear cluster's connectivity has been recently studied with zirconium MOFs but so far was not observed with RE-hexa-/nonanuclear clusters.[16]

As customary in RE chemistry, isolated reaction conditions for a given RE ion can be extrapolated effectively to other RE

DOI: 10.1021/jacs.5b00450
J. Am. Chem. Soc. 2015, 137, 5421−5430

metals and subsequently construct related isostructural RE-MOFs. Indeed, reactions between $Y(NO_3)_3{\cdot}6H_2O$ and $\mathbf{H_3L1}$, under similar reaction condition to **1**, resulted in the analogous Yttrium based **pek**-MOF-1 (**2**), formulated by SCXRD as $|(DMA)_7|[(Y_9(\mu_3\text{-}OH)_{12}(\mu_3\text{-}O)_2(H_2O)_9)(Y_6(\mu_3\text{-}OH)_8(2\text{-}FBzoate)_2(HCO_2)_2(DMF)_{0.67}(H_2O)_4)_3(\mathbf{L1})_{12}]{\cdot}(solv)_x$ (**2**); (DMA = dimethylammonium cations, solv = solvent, **L1** = $C_{15}H_7O_6$, 2-FBzoate = $C_7H_4FO_2$, DMF = C_3H_7NO).

The purity of compounds **1** and **2** was confirmed by similarities between the experimental and calculated powder X-ray diffraction (PXRD) patterns (Figures S1 and S2, Supporting Information). Additionally, both compounds show favorable water and thermal stability (Figures S3 and S6, Supporting Information), important attributes for the exploration of their associated porous system in relevant applications.

The **pek**-MOF-1 structure encloses cavities with a truncated hexagonal pyramidal-like contour and having diameters of 13.8 Å (height) and 9.8 Å (width) (in case of **1**), and accessible via two different apertures 4.9 and 7.6 Å. The said cage is derived from the hexagonal arrangement, in the equatorial plan, of six hexanuclear clusters and the capping by two nonanuclear clusters, in the two axial positions. Moreover, the structure has three intersecting infinite square channels with a kagome like motif and having an estimated diameter of 14.5 Å, taking van der Waals (vdW) radius into consideration (Figure S9, Supporting Information). The corresponding solvent accessible free volumes for **1** and **2** were estimated to be 58.6 and 59.4%, respectively, by summing voxels more than 1.2 Å away from the framework using PLATON software.[17]

Further structural analysis of the **pek**-MOF-1, revealed that each hexanuclear cluster is surrounded by four neighboring hexanuclear clusters to afford their subsequent arrangement in a 2-periodic sheet reminiscent of a kagome layer. The resultant kagome-like layers are further intercalated by a periodic array of nonanuclear clusters arranged in a hexagonal layer manner where each nonanuclear cluster superimposes with the two adjacent kagome hexagonal rings (Figure 2). Correspondingly, the **pek**-MOF structure can be regarded as built from pillared layers.

Specifically, when considering only the isophthalate moiety of the 3-c ligand, the structure now represents a regular AAA stacking of layers, made from 8-c hexanuclear clusters, bridged to four neighboring ones through two isophthalate ligands each time, and representing a well-known kagome (**kgm**) pattern (Figure 2). This can be related to the ubiquitous copper isophthalate **sql** and **kgm** layers found in many MOFs,[2,6,18] but in this case with a doubled connectivity of the MBBs (8 for the RE hexanuclear versus 4 for the Cu paddle wheel) resulting in doubly cross-linked **kgm** layers.

The resultant doubly cross-linked **kgm** layers are then pillared on top and bottom direction by the 12-c MBB, d6R, to form the overall (3,8,12)-c **pek** net. At this stage, the analogy can be made with two related nets based on the pillaring of simple **kgm** layers by 6-c nodes, **agw**[19] and **eef**,[2] where the vertex figures of the 6-c nodes match those from a trigonal prism and an octahedron, respectively. Unsurprisingly, the superimposition of **agw** or **eef** net with its corresponding mirror image net leads to the attainment of the **pek** net (Figure S10, Supporting Information). Credibly, the two 3-periodic nets (**agw** and **eef**) based on pillared 2-periodic **kgm** are regarded as suitable targets and ideal blueprints for the practice of the SBL approach toward directed assembly of MOFs.[2,19] Similarly, the **pek** net suggests the great potential to extend the SBL approach to doubly cross-linked layers in general and to the doubly cross-linked **kgm** layer in particular.

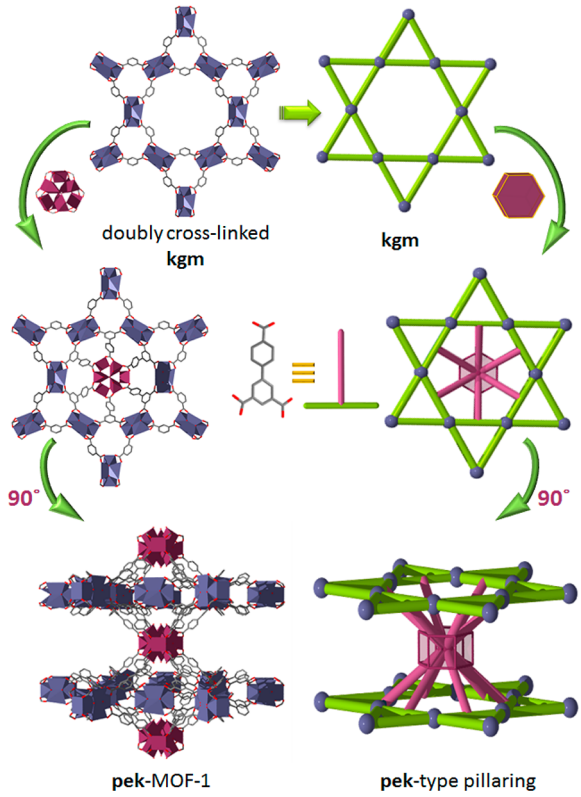

Figure 2. Schematic showing the new **pek**-type pillaring observed in **pek**-MOF-1.

In order to affirm the advocated SBL approach based on the doubly cross-linked **kgm** layer and associated **pek** topology, we designed and synthesized a suitable expanded ligand, 3-c tricarboxylate ligand, namely the 5-(4-carboxybenzyloxy)-isophthalic acid ($\mathbf{H_3L2}$). In contrast to the original ligand, $\mathbf{H_3L1}$, the isophthalate moiety believably responsible for the formation of the doubly cross-linked **kgm** layer is maintained while the 5-position of the isophthalate moiety is functionalized, providing a further elongated 3-c ligand than $\mathbf{H_3L1}$ (Figure 1).

As anticipated, reactions of $\mathbf{H_3L2}$ with Tb or Y nitrate salts, under similar conditions as **pek**-MOF-1, afforded colorless hexagonal crystals formulated by SCXRD studies as $|(DMA)_7|[(Tb_9(\mu_3\text{-}OH)_{12}(\mu_3\text{-}O)_2(H_2O)_9)(Tb_6(\mu_3\text{-}OH)_8(2\text{-}FBzoate)_2(HCO_2)_2(H_2O)_3)_3(\mathbf{L2})_{12}]{\cdot}(solv)_x$ (**3**) and $|(DMA)_7|[(Y_9(\mu_3\text{-}OH)_{12}(\mu_3\text{-}O)_2(H_2O)_9)(Y_6(\mu_3\text{-}OH)_8(2\text{-}FBzoate)_2(HCO_2)_2(DMF)_{1.66}(H_2O)_3)_3(\mathbf{L2})_{12}]{\cdot}(solv)_x$ (**4**), respectively ($\mathbf{L2}$ = $C_{16}H_9O_7$, 2-FBzoate = $C_7H_4FO_2$).

As envisioned, compounds **3** and **4** are isoreticular analogues of **pek**-MOF-1, named **pek**-MOF-2, constructed from the identical double **kgm** layers but at present connected together through elongated pillars, resulting in an increased spacing between the layers along the *c*-axis as evident by the observed increase in the c parameter (21.1 Å versus 26.4 Å in **pek**-MOF-1 and **pek**-MOF-2, respectively); (Figure S11, Supporting Information).

aea-**MOF Platform.** The evident association of the **pek**-MOF structure with the **kgm** layer has prompted us to explore other 3-c ligands that might disturb the formation of the requisite

DOI: 10.1021/jacs.5b00450
J. Am. Chem. Soc. 2015, 137, 5421−5430

kgm layer and prospectively, once again, promote the effect of the ligand geometrical attributes on the resulting topology.

Purposely, we opted to explore the carbazole-based ligands due to their associated contracted angle between the two carboxylate moieties, namely a 90° angle as compared to 120° in the isophthalate moiety.[20] Accordingly, the 9-(4-carboxyphenyl)-9*H*-carbazole-3,6-dicarboxylic acid (**H_3L3**) tricarboxylate ligand, which has 90° angle between carboxylate groups on the carbazole moiety, was designed and synthesized (Figure 1). Indeed, reactions of **H_3L3** with $Y(NO_3)_3{\cdot}6H_2O$, in the presence of the cluster directing agent 2-FBA, resulted in the formation of colorless hexagonal crystals, characterized and formulated by SCXRD and elemental microanalysis studies as $|(DMA)_{1.3}(Y_9(\mu_3\text{-}OH)_{12}(\mu_3\text{-}O)_2(Y_{1.2})(H_2O)_9(2\text{-}FBzoate)_{12})_{0.33}|[Y_9(Y_{0.28})(\mu_3\text{-}OH)_{12}(\mu_3\text{-}O)_2(H_2O)_9(Y_9(\mu_3\text{-}OH)_{12}(\mu_3\text{-}O)_2(H_2O)_9)_2(\mathbf{L3})_{12}]{\cdot}(solv)_x$ (**5**) (**L3** = $C_{15}H_7O_6$, 2-FBzoate = $C_7H_4FO_2$).

The SCXRD study discloses that compound **5** crystallizes in a primitive hexagonal space group *P6/mmm*. Analysis of the resultant crystal structure of **5** reveals the formation of a novel 3-periodic highly connected Y-MOF based solely on nonanuclear Y carboxylate-based clusters, formed *in situ*, and similar to the 12-c nonanuclear RE cluster observed in the **pek**-MOF. Specifically, the structure encloses three crystallographically independent nonanuclear clusters, each built by nine yttrium (Y) ions and capped by 12 carboxylate moieties, but only two of the nonanuclear clusters are copolymerized by the fully deprotonated tricarboxylate ligands (**L3**) to form a 3-periodic MOF hosting the third discrete nonanuclear cluster, capped by 12 carboxylate moieties from terminal 2-fluorobenzoate ligands, in its porous system.

From a topological analysis perspective, the two nonanuclear clusters, 12-connected MBBs, have the same d6R vertex figure as observed in the **pek**-MOF, but are topologically distinct and thus their assembly with the 3-c ligand reveals the discovery of a novel highly connected Y-MOF with a trinodal (3,12,12)-c net and **aea** underlying topology, Y-**aea**-MOF-1 (Figure 1). Analogous to the **pek** net, the new trinodal **aea** net is a minimal edge transitive net, transitivity [3244], and is an appropriate target for MOF crystal chemistry.

The purity of compounds **5** was confirmed by similarities between the experimental and calculated PXRD patterns (Figure S5, Supporting Information).

The **aea**-MOF-1 structure encloses a rhombic-like cage with estimated diameters of 9.2−13.7 Å (height) and 14.8 Å (width), taking vdW radius into consideration, having two separate apertures with relative dimensions of 5.2 × 3.5 Å and 10 × 5.4 Å. In addition, the structure possesses three intersecting infinite square channels with an estimated diameter of 12.5 Å (Figure S12, Supporting Information).

The corresponding solvent accessible free volume for **5** was estimated to be 55%, by summing voxels more than 1.2 Å away from the framework using PLATON software.[17]

Interestingly and similarly to the **pek**-MOF, the structure of **aea**-MOF-1 can be deconstructed into 2-periodic layers pillared by 12-c nonanuclear clusters. The layers are composed of one kind of nonanuclear clusters where each nonanuclear cluster is surrounded by three neighboring nonanuclear clusters, and linked in the plane, to afford their subsequent arrangement in a 2-periodic sheet reminiscent of a honeycomb (**hcb**) lattice. The resultant **hcb** layers are further intercalated by a periodic array of the second and distinct nonanuclear clusters arranged in a hexagonal layer manner where each nonanuclear cluster superimposes with the two adjacent hexagonal rings (Figure 3). Correspondingly, the **aea**-MOF structure can also be

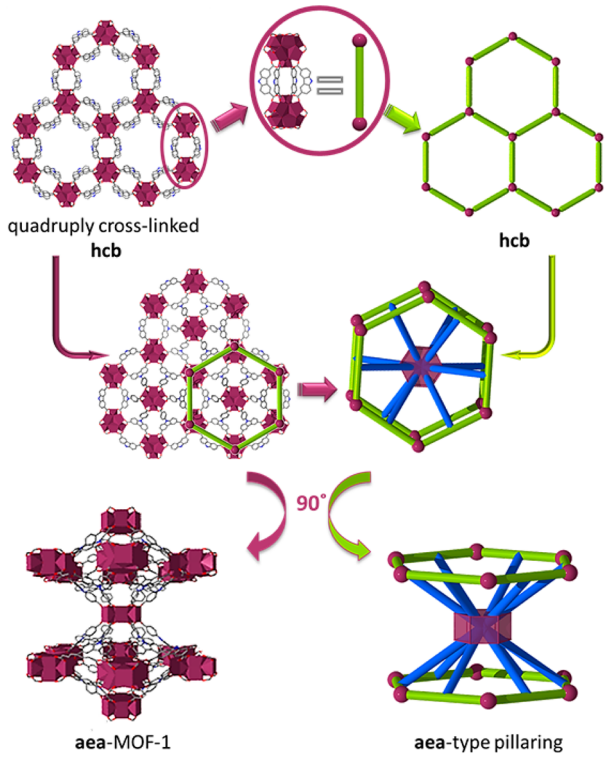

Figure 3. Schematic showing the **aea**-type pillaring observed in the **aea**-MOF-1.

regarded as built from pillared layers. Specifically, when considering only the carbazole dicarboxylate part of the 3-c ligand (i.e., discounting the connectivity via the benzoate moieties), it is possible to isolate some bidimensional layers, where each nonanuclear cluster is quadruply connected to each of three neighboring others via four carbazole dicarboxylate moieties (Figure 3). Topological simplification of the resultant 2-periodic arrangement reveals the occurrence of an **hcb** layer, considered in this case as a quadruply cross-linked **hcb**. We envision the newly discovered (3,12,12)-c **aea** net and the quadruply cross-linked **hcb** layer as promising blueprints for the directed assembly of highly connected and pillared MOFs using the SBL approach.

Gas Sorption Studies. In order to assess the porosity of the resultant **pek**- and **aea**-MOFs, and subsequently explore their potential for gas separations and gas storage, adsorption isotherms were collected using several probe molecules at various temperatures and pressures.

The Ar adsorption isotherm recorded at 87 K showed that **1** and **2** analogues of **pek**-MOF-1 exhibit fully reversible Type-I isotherm (Figure 4), indicative of a porous material with permanent microporosity. The apparent BET surface area and associated total pore volume were estimated to be 1330 $m^2\ g^{-1}$and 0.47 $cm^3\ g^{-1}$ for **1**, and 1608 $m^2\ g^{-1}$ and 0.58 $cm^3\ g^{-1}$ for **2**. The experimentally obtained total pore volumes are in excellent agreement with the associated theoretical values derived from SCXRD data, i.e., 0.47 $cm^3\ g^{-1}$ for **1** and 0.58 $cm^3\ g^{-1}$ for **2**. The pore size distribution (PSD) for **1** was assessed using the Ar adsorption data (Figure S15, Supporting Information) and revealed two type of pores with average sizes centered around 10 Å (cage) and 16.8 Å (channels),

DOI: 10.1021/jacs.5b00450
J. Am. Chem. Soc. 2015, 137, 5421−5430

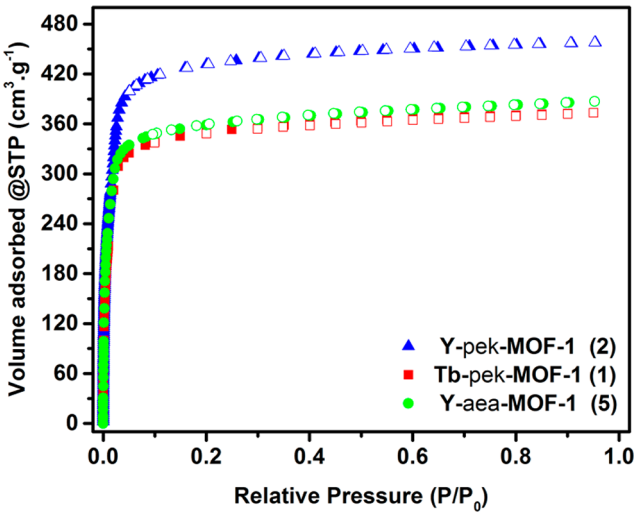

Figure 4. Ar adsorption isotherms for compounds **1**, **2** and **5** collected at 87 K.

which are in good qualitative agreement with the theoretical values derived from the associated crystal structure (8 and 13.5 Å, respectively). Akin porosity study based on Ar adsorption was performed on **5** (Figure 4) and presented an apparent BET surface area and a total pore volume of 1435 m^2 g^{-1} and 0.49 cm^3 g^{-1}, respectively. The PSD for **5** showed two distinct pores with diameters around 16 Å (cage) and 11 Å (channels) (Figure S16, Supporting Information), in good qualitative agreement with the theoretical values derived from the associated crystal structure (14, 12.5 Å, respectively).

In the light of our findings regarding the permanent porosity of **pek**-MOFs and **aea**-MOF-1, from both the theoretical and experimental point of view, we directed our efforts to the evaluation of the potential use of **pek**-MOF-1 in a number of energy relevant applications, such as CH_4 storage, CO_2 capture and light hydrocarbon separation. Examination of excess and absolute CH_4 gravimetric (cm^3 (STP) g^{-1}) and volumetric (cm^3 (STP) cm^{-3}) uptakes at intermediate and high pressures (Figure 5) showed that compound **2** and **1** methane uptakes are 150, 175 (RE = Y) and 140, 166 (RE = Tb) cm^3 (STP) cm^{-3} at 35 and 50 bar, respectively. The resulting CH_4 working storage capacities, assuming 35 bar (following the US Department of Energy standard)[21] or 50 bar as the highest adsorption pressure limit and 5 bar as the lowest desorption pressure limit, are estimated to be 110, 135 and 97, 123 cm^3 (STP) cm^{-3}, **2** and **1**, respectively. It is worth noting that for the volumetric uptakes calculation, the density of **pek**-MOFs was assumed to be constant and equivalent to the theoretical density derived from the fully evacuated associated crystal structure (1.02 and 1.25 g cm^{-3} for the **2** and **1** analogues, respectively). A comparative tabulated data for the best performing CH_4 storage MOFs is reported in Table S1 (Table S1, Supporting Information).

Figure 6a, displaying the volumetric CO_2 uptake for **pek**-MOFs in comparison with various relevant MOFs, shows that **2** and **1** exhibit a relatively very high volumetric CO_2 uptake at 25 bar and 298 K. Specifically, the **2** exhibits CO_2 uptake of 288 cm^3 (STP) cm^{-3} that is slightly higher than MOF-177 (273 cm^3 (STP) cm^{-3}),[22] HKUST-1 (276 cm^3 (STP) cm^{-3}),[23] Mg-MOF-74 (285 cm^3 (STP) cm^{-3}),[24] MOF-5 (225 cm^3 (STP)

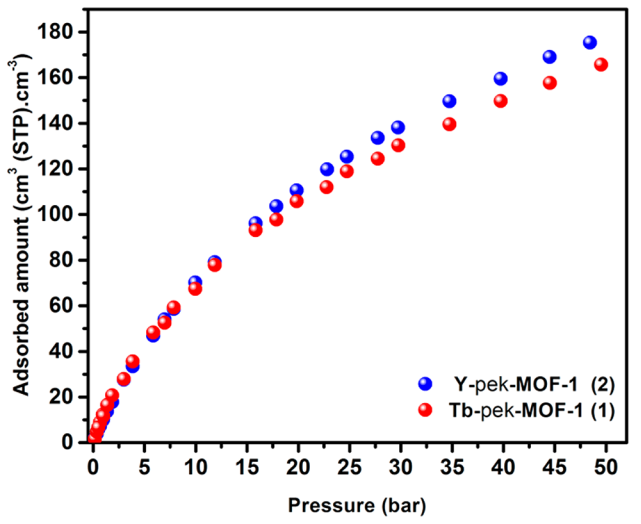

Figure 5. Absolute CH_4 adsorption isotherms of compounds **1** and **2** at 298 K and up to 50 bar.

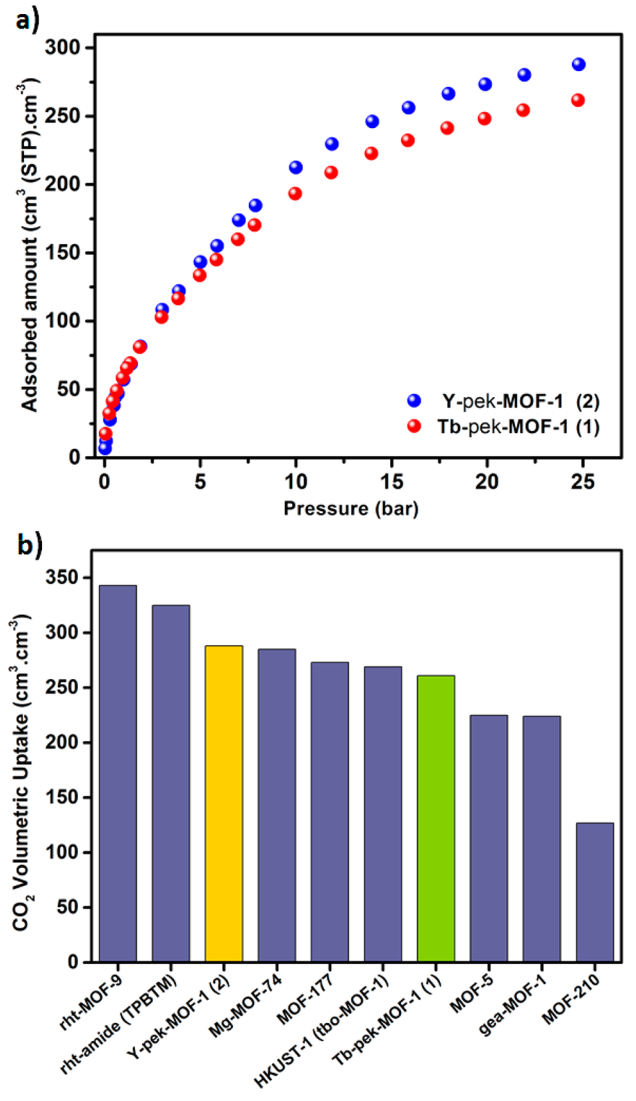

Figure 6. (a) Absolute adsorption isotherms of CO_2 at 298 K and up to 25 bar for **1** and **2**. (b) Comparison of CO_2 uptake at 25 bar and 298 K for **pek**-MOFs and the best performing MOFs available in the literature, to the best of our knowledge.

DOI: 10.1021/jacs.5b00450
J. Am. Chem. Soc. 2015, 137, 5421−5430

cm^{-3}),[22] **gea**-MOF-1 (224 cm^3 (STP) cm^{-3}),[5c] MOF-210 (127 cm^3 (STP) cm^{-3}),[22] MOF-200 (112 cm^3 (STP) cm^{-3})[22] but lower than **rht**-MOF-amide (*N*,*N*,*N*′′-tris(isophthalyl)-1,3,5-benzenetricarboxamide, TPBTM) (325 cm^3 (STP) cm^{-3})[25] and **rht**-MOF-9 (343 cm^3 (STP) cm^{-3}).[26] **1** was found to uptake a relatively reduced CO_2 (261 cm^3 (STP) cm^{-3}). These outstanding CO_2 volumetric uptakes for the RE-**pek**-MOF-1 at 25 bar could be explained by the combination of high porosity and high localized charge density, induced by the presence of both the nonanuclear and hexanuclear clusters, and the pending 2-fluorobenzoate moieties in the cavities. This combined effect led to moderate CO_2-framework interactions in the range of 38−32 kJ mol^{-1} at low CO_2 loading (Figures S17 and S18, Supporting Information) but a relatively high uptakes/density of CO_2 in the framework of RE-**pek**-MOF-1.

With the particular open structure of RE-**pek**-MOF-1 and its associated low uptakes of H_2, and CH_4 at low pressures, indicative of reasonably weak sorbate-framework interactions/affinity, (Figures S19 and S20, Supporting Information) as compared to larger and highly polarizable probe molecules (Figure 7a), we found it compelling to explore the potential of **1** for the removal of hydrocarbons from relevant gas streams. Condensable gases such as C_3H_8 and *n*-C_4H_{10} present in gas streams containing valuable commodities such as H_2 and CH_4 are undesirable and need to be subsequently removed. Accordingly, in addition to CO_2, single gas adsorption properties of C_2H_6, C_3H_8 and *n*-C_4H_{10} were investigated at 298 K and confronted with the corresponding properties of H_2 and CH_4.

It is worth noting that our group recently reported on the great potential of MOFs for light hydrocarbon separation.[5c,27] Interestingly, the CO_2, C_2H_6, C_3H_8 and *n*-C_4H_{10} adsorption isotherms were reasonably much steeper at low pressures than those for CH_4 and H_2, indicative of the preferential adsorption affinity for **1**, particularly to C_3H_8 and *n*-C_4H_{10} versus H_2 and CH_4. Examination of single gas adsorption data using Ideal Adsorption Solution Theory (IAST) confirmed that **1** exhibits high adsorption selectivity for various gas pair systems such as C_3H_8/CH_4 and *n*-C_4H_{10}/CH_4 (Figure 7b). Because of the insignificant uptakes of H_2 on **1** at 298 K, adequate prediction of C_3H_8/H_2, *n*-C_4H_{10}/CH_2 and CO_2/H_2 was not possible. Nevertheless, the less selective adsorption of H_2 when compared to CH_4 presents the **pek**-MOFs as excellent candidates for H_2 separation/purification. Therefore, **pek**-MOFs can be employed as separation agents for production of these valuable commodities (H_2 and CH_4) from many gas streams relevant to natural gas, biogas and petrochemical industry.

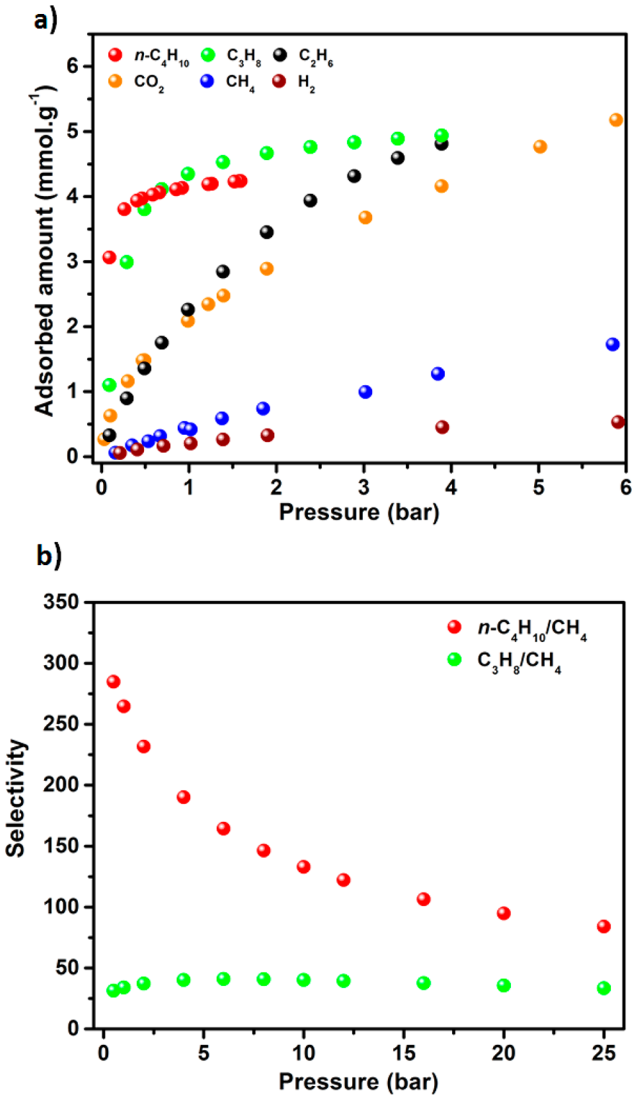

Figure 7. (a) CO_2, CH_4, H_2, C_2H_6, C_3H_8 and *n*-C_4H_{10} single gas adsorption at 298 K for **1**, (b) Separation factor of C_3H_8 (5%) and *n*-C_4H_{10} (5%) in binary mixture with CH_4 (95%).

CONCLUSIONS

We reported here the discovery of two fascinating and highly connected nets having novel **pek** and **aea** topologies via a systematic exploration on the use of RE metal salts in combination with relatively less symmetrical 3-c tricarboxylate ligands instead of the parent symmetrical tricarboxylate ligand, H_3BTB. The implemented relatively lower symmetry of the 3-c tricarboxylate ligand was presumably responsible in driving the simultaneous occurrence of nonanuclear $[RE_9(\mu_3\text{-}OH)_{12}(\mu_3\text{-}O)_2(O_2C\text{-})_{12}]$ and hexanuclear $[RE_6(OH)_8(O_2C\text{-})_8]$ carboxylate-based clusters to form novel 3-periodic **pek**-MOFs. Subsequent use of another 3-c tricarboxylate ligand with further contracted angles between the carboxylates (from 120° to 90°) led to the formation of a second highly connected net, (3,12,12)-c with an unprecedented **aea** topology. Notably, **pek**-MOF and **aea**-MOF are so far the first examples of RE-MOFs containing 12-c d6R SBUs which are exceptionally promising building units for the practice of reticular chemistry and subsequently the design of new highly connected MOFs. The **pek**-MOF and **aea**-MOF are also the first examples of pillar-based MOFs where pillars manifest a relatively high connectivity (12-c), a unique feature that offer potential for the practice of the SBL approach for the design and directed assembly of highly connected MOFs. The exceptional structural features of **pek**-MOFs were directly concomitant with their excellent CH_4, CO_2 storage properties as well as their promising gas separation potential for gas pair systems such as C_3H_8/CH_4, *n*-C_4H_{10}/CH_4 relevant to natural gas upgrading. There is no doubt that the ongoing design and development of finely tailored isoreticular **pek** and **aea** MOFs using the SBL approach will lead to enhanced gas storage and gas/vapor separation properties. Accordingly, work is in progress to construct isoreticular MOFs based on **pek** and **aea** topologies from various functional ligands.

DOI: 10.1021/jacs.5b00450
J. Am. Chem. Soc. 2015, 137, 5421−5430

EXPERIMENTAL SECTION

Materials and Methods. Details on the synthesis of organic ligands used in this study, biphenyl-3,4,5-tricarboxylic acid (H_3**L1**), 5-(4-carboxybenzyloxy)isophthalic acid (H_3**L2**) and 9-(4-carboxyphenyl)-9H-carbazole-3,6-dicarboxylic acid (H_3**L3**) are provided in the Supporting Information.

Single-crystal X-ray diffraction data were collected using a Bruker-AXS SMART-APEX2 CCD diffractometer (Cu Kα, λ = 1.54178 Å). Fourier-transform infrared (FT-IR) spectra (4000−600 cm^{-1}) were collected in the solid state on a Nicolet 700 FT-IR spectrometer. The peak intensities are described in each of the spectra as very strong (vs), strong (s), medium (m), weak (w), broad (br) and shoulder (sh). Elemental analysis was performed with a Thermo Scientific Flash 2000 instrument. Powder X-ray diffraction (PXRD) measurements were performed on a PANalytical X'Pert PRO MPD X-ray diffractometer at 45 kV, 40 mA for Cu Kα (λ = 1.5418 Å) equipped with a variable-temperature stage, with a scan speed of 20/min. The sample was held at the designated temperatures for at least 10 min between each scan. High resolution dynamic thermal gravimetric analysis (TGA) were performed under a continuous N_2 flow and recorded on a TA Instruments hi-res TGAQ500 thermal gravimetric analyzer. Low pressure gas sorption measurements were performed on a fully automated Autosorb-iQ gas sorption analyzer (Quantachrome Instruments) and a fully automated micropore gas analyzer 3Flex Analyzer (Micromeritics Instruments). High pressure gas sorption studies were performed on a magnetic suspension balance marketed by Rubotherm (Germany).

Synthesis of Compounds. *Synthesis of* ***1*** *(Tb-**pek**-MOF-1).* A solution of $Tb(NO_3)_3{\cdot}5H_2O$ (29 mg, 0.068 mmol), H_3**L1** (3.4 mg, 0.012 mmol), 2-fluorobenzoic acid (285 mg, 2.04 mmol) in *N*,*N*-dimethylformamide (DMF) (3 mL), H_2O (2 mL) and chlorobenzene (1 mL), was prepared in a 20 mL scintillation vial and subsequently heated to 105 °C for 72 h to give pure colorless hexagonal crystals. Crystals of **1** were harvested, washed with MeOH and air-dried. FT-IR (4000−650 cm^{-1}): 3349 (br), 1611 (vs), 1574 (vs), 1438 (s), 1400 (vs), 1297 (w), 1252 (w), 1100 (w), 1018 (w), 871 (w), 776 (s), 761 (s), 713 (s). Elemental Analysis: C = 28.2% (theo: 29.9%), H = 3.0% (2.7%), N = 2.3% (1.9%).

Synthesis of ***2*** *(Y-**pek**-MOF-1).* A solution of $Y(NO_3)_3{\cdot}6H_2O$ (39 mg, 0.102 mmol), H_3**L1** (5 mg, 0.018 mmol), 2-fluorobenzoic acid (428 mg, 3.06 mmol) in DMF (4.5 mL), H_2O (3 mL) and chlorobenzene (1.5 mL), was prepared in a 20 mL scintillation vial and subsequently heated to 105 °C for 72 h to give pure colorless hexagonal crystals. Crystals of **2** were harvested, washed with MeOH and air-dried. FT-IR (4000−650 cm^{-1}): 2818 (br), 1612 (s), 1487 (w), 1465 (w), 1454 (w), 1407 (vs), 1305 (vs), 1225 (s), 1162 (w), 1135 (w), 1088 (w), 1033 (w), 918 (w), 869 (w), 844 (w), 793 (w), 751 (s), 714 (w), 687 (w). Elemental Analysis: C = 35.1% (theo: 36.5%), H = 3.5% (3.3%), N = 2.2% (2.3%).

Synthesis of ***3*** *(Tb-**pek**-MOF-2).* A solution of $Tb(NO_3)_3{\cdot}5H_2O$ (44 mg, 0.102 mmol), H_3**L2** (5.6 mg, 0.018 mmol), 2-fluorobenzoic acid (336 mg, 2.4 mmol) in DMF (4.5 mL), H_2O (3 mL) and chlorobenzene (1.5 mL), was prepared in a 20 mL scintillation vial and subsequently heated to 105 °C for 72 h to give pure colorless hexagonal crystals. Crystals of **3** were harvested, washed with MeOH and air-dried. FT-IR (4000−650 cm^{-1}): 3331 (br), 1593 (s), 1557 (s), 1449 (s), 1379 (vs), 1322 (s), 1265 (w), 1179 (w), 1129 (w), 1100 (w), 1036 (w), 1019 (w), 996 (w), 961 (w), 918 (w), 859 (w), 811 (w), 775 (s), 709 (s). Elemental Analysis: C = 29.5% (theo: 29.9%), H = 2.5% (2.8%), N = 1.9% (1.8%).

Synthesis of ***4*** *(Y-**pek**-MOF-2).* A solution of $Y(NO_3)_3{\cdot}6H_2O$ (26 mg, 0.068 mmol), H_3**L2** (2 mg, 0.006 mmol), 2-fluorobenzoic acid (224 mg, 1.6 mmol) in DMF (2.15 mL), H_2O (2 mL) and chlorobenzene (1 mL), was prepared in a 20 mL scintillation vial and subsequently heated to 105 °C for 5 days to give pure colorless hexagonal crystals. Crystals of **4** were harvested, washed with MeOH and air-dried. FT-IR (4000−650 cm^{-1}): 3422 (br), 2931 (w), 1621 (s), 1565 (s), 1496 (w), 1437 (w), 1407 (s), 1407 (s), 1386 (vs), 1320 (w), 1255 (s), 1178 (w), 1129 (w), 1096 (s), 1060 (w), 1020 (w), 995 (w), 962 (w), 890 (w), 865 (w), 812 (w), 780 (s), 709 (s). Elemental Analysis: C = 32.2% (theo: 36.6%), H = 3.4% (3.4%), N = 2.3% (2.2%).

Synthesis of ***5*** *(Y-**aea**-MOF-1).* A solution of $Y(NO_3)_3{\cdot}6H_2O$ (21.5 mg, 0.056 mmol), H_3**L3** (3.8 mg, 0.01 mmol), 2-fluorobenzoic acid (420 mg, 3 mmol) in DMF (4 mL), H_2O (2 mL) and chlorobenzene (1 mL), was prepared in a 20 mL scintillation vial and subsequently heated to 105 °C for 2 days to give pure colorless hexagonal crystals. Crystals of **5** were harvested, washed with MeOH and air-dried. FT-IR (4000−650 cm^{-1}): 1591 (s), 1545 (s), 1496 (w), 1398 (vs), 1277 (s), 779 (s), 709 (w). Elemental Analysis: C = 36.4% (theo: 36.4%), H = 2.4% (2.1%), N = 1.9% (3.2%)

ASSOCIATED CONTENT

Supporting Information

Synthesis of organic ligands, PXRD, additional structural figures, sorption, and single-crystal X-ray diffraction data (CIF). This material is available free of charge via the Internet at http://pubs.acs.org.

AUTHOR INFORMATION

Corresponding Author

*mohamed.eddaoudi@kaust.edu.sa

Notes

The authors declare no competing financial interest.

ACKNOWLEDGMENTS

Research reported in this publication was supported by King Abdullah University of Science and Technology (KAUST).

REFERENCES

(1) (a) Eddaoudi, M.; Moler, D. B.; Li, H.; Chen, B.; Reineke, T. M.; O'Keeffe, M.; Yaghi, O. M. *Acc. Chem. Res.* **2001**, *34*, 319−330. (b) Eddaoudi, M.; Kim, J.; Rosi, N.; Vodak, D.; Wachter, J.; O'Keeffe, M.; Yaghi, O. M. *Science* **2002**, *295*, 469−472. (c) Long, J. R.; Yaghi, O. M. *Chem. Soc. Rev.* **2009**, *38*, 1201−1508. (d) Zhou, H.-C.; Long, J. R.; Yaghi, O. M. *Chem. Rev.* **2012**, *112*, 673−1268. (e) Zhou, H.-C.; Kitagawa, S. *Chem. Soc. Rev.* **2014**, *43*, 5403−6176. (f) Horcajada, P.; Chalati, T.; Serre, C.; Gillet, B.; Sebrie, C.; Baati, T.; Eubank, J. F.; Heurtaux, D.; Clayette, P.; Kreuz, C.; Chang, J.-S.; Hwang, Y. K.; Marsaud, V.; Bories, P.-N.; Cynober, L.; Gil, S.; Férey, G.; Couvreur, P.; Gref, R. *Nat. Mater.* **2010**, *9*, 172−178.

(2) Guillerm, V.; Kim, D.; Eubank, J. F.; Luebke, R.; Liu, X.; Adil, K.; Lah, M. S.; Eddaoudi, M. *Chem. Soc. Rev.* **2014**, *43*, 6141−6172.

(3) O'Keeffe, M.; Yaghi, O. M. *Chem. Rev.* **2012**, *112*, 675−702.

(4) O'Keeffe, M.; Peskov, M. A.; Ramsden, S. J.; Yaghi, O. M. *Acc. Chem. Res.* **2008**, *41*, 1782−1789.

(5) (a) Nouar, F.; Eubank, J. F.; Bousquet, T.; Wojtas, Ł.; Zaworotko, M. J.; Eddaoudi, M. *J. Am. Chem. Soc.* **2008**, *130*, 1833−1835. (b) Eubank, J. F.; Nouar, F.; Luebke, R.; Cairns, A. J.; Wojtas, Ł.; Alkordi, M.; Bousquet, T.; Hight, M. R.; Eckert, J.; Embs, J. P.; Georgiev, P. A.; Eddaoudi, M. *Angew. Chem., Int. Ed.* **2012**, *51*, 10099−10103. (c) Guillerm, V.; Weseliński, Ł. J.; Belmabkhout, Y.; Cairns, A. J.; D'Elia, V.; Wojtas, L.; Adil, K.; Eddaoudi, M. *Nat. Chem.* **2014**, *6*, 673−680.

(6) (a) Eubank, J. F.; Wojtas, Ł.; Hight, M. R.; Bousquet, T.; Kravtsov, V. C.; Eddaoudi, M. *J. Am. Chem. Soc.* **2011**, *133*, 17532−17535. (b) Eubank, J. F.; Mouttaki, H.; Cairns, A. J.; Belmabkhout, Y.; Wojtas, Ł.; Luebke, R.; Alkordi, M.; Eddaoudi, M. *J. Am. Chem. Soc.* **2011**, *133*, 14204−14207.

(7) (a) Cavka, J. H.; Jakobsen, S.; Olsbye, U.; Guillou, N.; Lamberti, C.; Bordiga, S.; Lillerud, K. P. *J. Am. Chem. Soc.* **2008**, *130*, 13850−13851. (b) Dan-Hardi, M.; Serre, C.; Frot, T.; Rozes, L.; Maurin, G.; Sanchez, C.; Férey, G. *J. Am. Chem. Soc.* **2009**, *131*, 10857−10859. (c) Guillerm, V.; Gross, S.; Serre, C.; Devic, T.; Bauer, M.; Férey, G. *Chem. Commun.* **2010**, *46*, 767−769. (d) Guillerm, V.; Ragon, F.; Dan-Hardi, M.; Devic, T.; Vishnuvarthan, M.; Campo, B.; Vimont, A.; Clet,

DOI: 10.1021/jacs.5b00450
J. Am. Chem. Soc. 2015, 137, 5421−5430

G.; Yang, Q.; Maurin, G.; Férey, G.; Vittadini, A.; Gross, S.; Serre, C. *Angew. Chem., Int. Ed.* **2012**, *51*, 9267−71. (e) Morris, W.; Volosskiy, B.; Demir, S.; Gandara, F.; McGrier, P. L.; Furukawa, H.; Cascio, D.; Stoddart, J. F.; Yaghi, O. M. *Inorg. Chem.* **2012**, *51*, 6443−6445. (f) Yang, Q.; Guillerm, V.; Ragon, F.; Wiersum, A. D.; Llewellyn, P. L.; Zhong, C.; Devic, T.; Serre, C.; Maurin, G. *Chem. Commun.* **2012**, *48*, 9831−9833. (g) Du, D.-Y.; Qin, J.-S.; Sun, Z.; Yan, L.-K.; O'Keeffe, M.; Su, Z.-M.; Li, S.-L.; Wang, X.-H.; Wang, X.-L.; Lan, Y.-Q. *Sci. Rep.* **2013**, *3*, 2616. (h) Xue, D.-X.; Cairns, A. J.; Belmabkhout, Y.; Wojtas, Ł.; Liu, Y.; Alkordi, M. H.; Eddaoudi, M. *J. Am. Chem. Soc.* **2013**, *135*, 7660−7667. (i) Ahnfeldt, T.; Moellmer, J.; Guillerm, V.; Staudt, R.; Serre, C.; Stock, N. *Chem.—Eur. J.* **2011**, *17*, 6462−6468. (j) Vaesen, S.; Guillerm, V.; Yang, Q.; Wiersum, A. D.; Marszalek, B.; Gil, B.; Vimont, A.; Daturi, M.; Devic, T.; Llewellyn, P. L.; Serre, C.; Maurin, G.; De Weireld, G. *Chem. Commun.* **2013**, *49*, 10082−10084.

(8) (a) Schaate, A.; Roy, P.; Godt, A.; Lippke, J.; Waltz, F.; Wiebcke, M.; Behrens, P. *Chem.—Eur. J.* **2011**, *17*, 6643−6651. (b) Umemura, A.; Diring, S.; Furukawa, S.; Uehara, H.; Tsuruoka, T.; Kitagawa, S. *J. Am. Chem. Soc.* **2011**, *133*, 15506−15513.

(9) (a) Roy, S.; Chakraborty, A.; Maji, T. K. *Coord. Chem. Rev.* **2014**, *273*−*274*, 139−164. (b) Park, Y. K.; Choi, S. B.; Kim, H.; Kim, K.; Won, B.-H.; Choi, K.; Choi, J.-S.; Ahn, W.-S.; Won, N.; Kim, S.; Jung, D. H.; Choi, S.-H.; Kim, G.-H.; Cha, S.-S.; Jhon, Y. H.; Yang, J. K.; Kim, J. *Angew. Chem., Int. Ed.* **2007**, *46*, 8230−8233. (c) Luo, J.; Xu, H.; Liu, Y.; Zhao, Y.; Daemen, L. L.; Brown, C.; Timofeeva, T. V.; Ma, S.; Zhou, H.-C. *J. Am. Chem. Soc.* **2008**, *130*, 9626−9627. (d) Guillou, O.; Daiguebonne, C. Lanthanide-containing coordination polymers. In *Handbook on the Physics and Chemistry of Rare Earths*; Elsevier: Amsterdam, 2005; Vol. *34*, pp 359−404. (e) Devic, T.; Serre, C.; Audebrand, N.; Marrot, J.; Férey, G. *J. Am. Chem. Soc.* **2005**, *127*, 12788−12789.

(10) Luebke, R.; Belmabkhout, Y.; Weseliński, Ł. J.; Cairns, A. J.; Norton, G.; Alkordi, M.; Wojtas, Ł.; Adil, K.; Eddaoudi, M. *Chemical Science* **2015**, DOI: 10.1039/C5SC00614G.

(11) (a) Rosi, N. L.; Eddaoudi, M.; Kim, J.; O'Keeffe, M.; Yaghi, O. M. *CrystEngComm* **2002**, *4*, 401−404. (b) Brunner, G. O. *Z. Kristallogr.* **1981**, *156*, 295−303.

(12) (a) Lin, Z.-J.; Xu, B.; Liu, T.-F.; Cao, M.-N.; Lü, J.; Cao, R. *Eur. J. Inorg. Chem.* **2010**, *2010*, 3842−3849. (b) Guo, Z.; Xu, H.; Su, S.; Cai, J.; Dang, S.; Xiang, S.; Qian, G.; Zhang, H.; O'Keeffe, M.; Chen, B. *Chem. Commun.* **2011**, *47*, 5551−5553. (c) Hao, Z.; Yang, G.; Song, X.; Zhu, M.; Meng, X.; Zhao, S.; Song, S.; Zhang, H. *J. Mater. Chem. A* **2014**, *2*, 237−244. (d) Yan, D.; Duan, Q. *Inorg. Chem. Commun.* **2013**, *36*, 188−191. (e) Li, X.-Y.; Lin, Z.-J.; Yang, Y.-Y.; Cao, R. *CrystEngComm* **2014**, *16*, 6425−6432.

(13) Eddaoudi, M.; Sava, D. F.; Eubank, J. F.; Adil, K.; Guillerm, V. *Chem. Soc. Rev.* **2015**, *44*, 228−249.

(14) Allen, F. H. *Acta Crystallogr., Sect. B: Struct. Sci.* **2002**, *58*, 380−388.

(15) Feng, D.; Gu, Z.-Y.; Chen, Y.-P.; Park, J.; Wei, Z.; Sun, Y.; Bosch, M.; Yuan, S.; Zhou, H.-C. *J. Am. Chem. Soc.* **2014**, *136*, 17714−17717.

(16) (a) Morris, W.; Volosskiy, B.; Demir, S.; Gándara, F.; McGrier, P. L.; Furukawa, H.; Cascio, D.; Stoddart, J. F.; Yaghi, O. M. *Inorg. Chem.* **2012**, *51*, 6443−6445. (b) Feng, D.; Gu, Z.-Y.; Li, J.-R.; Jiang, H.-L.; Wei, Z.; Zhou, H.-C. *Angew. Chem., Int. Ed.* **2012**, *51*, 10307−10310. (c) Bon, V.; Senkovska, I.; Baburin, I. A.; Kaskel, S. *Cryst. Growth Des.* **2013**, *13*, 1231−1237. (d) Mondloch, J. E.; Bury, W.; Fairen-Jimenez, D.; Kwon, S.; DeMarco, E. J.; Weston, M. H.; Sarjeant, A. A.; Nguyen, S. T.; Stair, P. C.; Snurr, R. Q.; Farha, O. K.; Hupp, J. T. *J. Am. Chem. Soc.* **2013**, *135*, 10294−10297.

(17) Spek, A. L. *Acta Crystallogr., Sect. A: Found. Crystallogr.* **1990**, *A46*, c34.

(18) (a) He, Y.; Li, B.; O'Keeffe, M.; Chen, B. *Chem. Soc. Rev.* **2014**, *43*, 5618−5656. (b) Yan, Y.; Yang, S.; Blake, A. J.; Schröder, M. *Acc. Chem. Res.* **2013**, *47*, 296−307.

(19) (a) Wong-Foy, A. G.; Lebel, O.; Matzger, A. J. *J. Am. Chem. Soc.* **2007**, *129*, 15740−15741. (b) Schnobrich, J. K.; Lebel, O.; Cychosz, K. A.; Dailly, A.; Wong-Foy, A. G.; Matzger, A. J. *J. Am. Chem. Soc.* **2010**, *132*, 13941−13948.

(20) Weseliński, Ł. J.; Luebke, R.; Eddaoudi, M. *Synthesis* **2014**, *46*, 596−599.

(21) Peng, Y.; Krungleviciute, V.; Eryazici, I.; Hupp, J. T.; Farha, O. K.; Yildirim, T. *J. Am. Chem. Soc.* **2013**, *135*, 11887−11894.

(22) Furukawa, H.; Ko, N.; Go, Y. B.; Aratani, N.; Choi, S. B.; Choi, E.; Yazaydin, A. Ö.; Snurr, R. Q.; O'Keeffe, M.; Kim, J.; Yaghi, O. M. *Science* **2010**, *329*, 424−428.

(23) Moellmer, J.; Moeller, A.; Dreisbach, F.; Glaeser, R.; Staudt, R. *Microporous Mesoporous Mater.* **2011**, *138*, 140−148.

(24) Simmons, J. M.; Wu, H.; Zhou, W.; Yildirim, T. *Energy Environ. Sci.* **2011**, *4*, 2177−2185.

(25) Zheng, B.; Bai, J.; Duan, J.; Wojtas, L.; Zaworotko, M. J. *J. Am. Chem. Soc.* **2010**, *133*, 748−751.

(26) Luebke, R.; Weseliński, Ł. J.; Belmabkhout, Y.; Chen, Z.; Wojtas, L.; Eddaoudi, M. *Cryst. Growth Des.* **2014**, *14*, 414−418.

(27) Belmabkhout, Y.; Mouttaki, H.; Eubank, J. F.; Guillerm, V.; Eddaoudi, M. *RSC Adv.* **2014**, *4*, 63855−63859.

DOI: 10.1021/jacs.5b00450
J. Am. Chem. Soc. 2015, 137, 5421−5430